Bioorganic & Medicinal Chemistry 18 (2010) 5885–5895

Contents lists available at ScienceDirect

Bioorganic & Medicinal Chemistry

journal homepage: www.elsevier.com/locate/bmc

Characterization of new PPARγ agonists: Benzimidazole derivatives—importance of positions 5 and 6, and computational studies on the binding mode

Matthias Goebel [a], Gerhard Wolber [a], Patrick Markt [b], Bart Staels [c], Thomas Unger [d], Ulrich Kintscher [d], Ronald Gust [a,e,*]

[a] Institute of Pharmacy, Freie Universität Berlin, Königin-Luise Strasse 2+4, 14195 Berlin, Germany
[b] Center for Molecular Biosciences and Institute of Pharmacy, Department of Pharmaceutical Chemistry, Computer-Aided Molecular Design Group, University of Innsbruck, Innrain 52c, 6020 Innsbruck, Austria
[c] INSERM U545, Institut Pasteur de Lille, Faculté de Pharmacie et Faculté de Médecine, Université de Lille 2, 59000 Lille, France
[d] Center for Cardiovascular Research (CCR), Institute of Pharmacology, Charité-Universitätsmedizin Berlin, Hessische Strasse 3-4, 10115 Berlin, Germany
[e] Institute of Pharmacy, Department of Pharmaceutical Chemistry, University of Innsbruck, Innrain 52c, 6020 Innsbruck, Austria

ARTICLE INFO

Article history:
Received 5 November 2009
Revised 28 June 2010
Accepted 29 June 2010
Available online 3 July 2010

Keywords:
Benzimidazole derivatives
Partial agonism
Selective PPARγ modulators
Structure–activity relationship
Molecular modeling

ABSTRACT

In this and previous studies we investigated the importance of partial structures of Telmisartan on PPARγ activation. The biphenyl-4-ylmethyl moiety at N1 and residues at C2 of the central benzimidazole were identified to be essential for receptor activation and potency of receptor binding. Now we focused our attention on positions 5 and 6 of the central benzimidazole and introduced bromine (**3b**–**5**/**6**, **3c**), phenylcarbonyl (**3d**–**5**/**6**), hydroxy(phenyl)methyl (**3g**–**5**/**6**), hydroxymethyl (**3h**–**5**/**6**) and formyl (**3i**) groups. The selection of these moieties was inspired by the structure of Losartan and its metabolite EXP3179. In order to increase the hydrophobicity of the central part of the molecule, the benzimidazole was exchanged by a naphtho[2,3-*d*]imidazole (**5**). The compounds **3a**–**3i** and **5** were tested in a differentiation assay using 3T3-L1 preadipocytes and a luciferase assay using COS-7 cells, transiently transfected with pGal4-hPPARγDEF, pGal5-TK-pGL3 and pRL-CMV, as established models for the assessment of cellular PPARγ activation. An enhanced effect on PPARγ activation could be observed if lipophilic moieties are introduced in these positions. 4′-[(2-Propyl-1*H*-naphtho[2,3-*d*]imidazol-1-yl)methyl]biphenyl-2-carboxylic acid (**5**) was identified as the most potent compound with an EC_{50} of 0.26 μM and the profile of a full agonist.

Together with compounds of the former structure–activity relationship study (position 2-substituted benzimidazole derivatives **4a**–**4j**), the binding mode of Telmisartan and its derivatives have been analyzed in 3D pharmacophore-driven docking experiments.

1. Introduction

The Peroxisome Proliferator-Activated Receptor γ (PPARγ) is a major regulator of adipogenesis and also involved in glucose homoeostasis, cell differentiation and inflammation.[1,2] The receptor belongs to the nuclear receptor superfamily of ligand-activated transcription factors.[3–6] Glitazones or thiazolidinediones, such as Pioglitazone or Rosiglitazone, are high affinity ligands and full agonists for this receptor and are currently used in the treatment of type 2 diabetes mellitus. Because of the side effects of glitazones such as weight gain, edema and fluid retention, the characterization of new PPARγ ligands that retain metabolic efficacy without exerting adverse actions plays a central role in the development of new therapeutic strategies for insulin resistance and type 2 diabetes mellitus.[7] A promising new group of such ligands are selective PPARγ modulators (SPPARγMs), compounds that activate only a subset of the functions induced by cognate ligands or act in a cell-type selective manner.[8] It has been shown that a subgroup of angiotensin II receptor blockers (ARBs) induced PPARγ activity, among which Telmisartan showed the highest activating properties.[9,10] In addition, there is accumulating evidence for Telmisartan and Irbesartan to act like SPPARγMs.[11]

We already demonstrated in a previous study that a 'backbone' part of Telmisartan containing the basic scaffold of the 1-(biphenyl-4-ylmethyl)-1*H*-benzimidazole seems to be absolutely necessary to maintain PPARγ activation (Fig. 1).[12] Furthermore, the alkyl chain in position 2 of the benzimidazole core, especially the

* Corresponding author. Address: Institut für Pharmazie, Abteilung für Pharmazeutische Chemie, Universität Innsbruck, Innrain 52c, 6020 Innsbruck, Austria. Tel.: +43 512 507 5245; fax: +43 512 507 2940.
E-mail addresses: ronald.gust@uibk.ac.at, rgust@zedat.fu-berlin.de (R. Gust).

0968-0896/$ - see front matter © 2010 Elsevier Ltd. All rights reserved.
doi:10.1016/j.bmc.2010.06.102

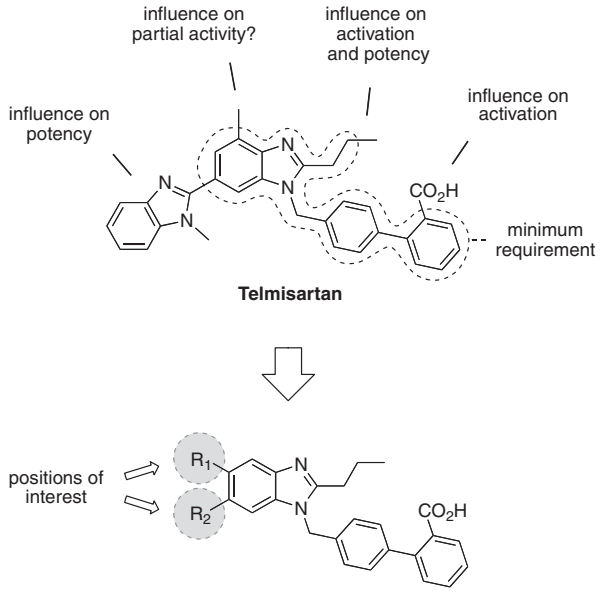

Figure 1. Central 1-(biphenyl-4-ylmethyl)-1*H*-benzimidazole structure of Telmisartan as a basis for new PPARγ ligands with the focus of interest on position 5 and 6 of the benzimidazole.

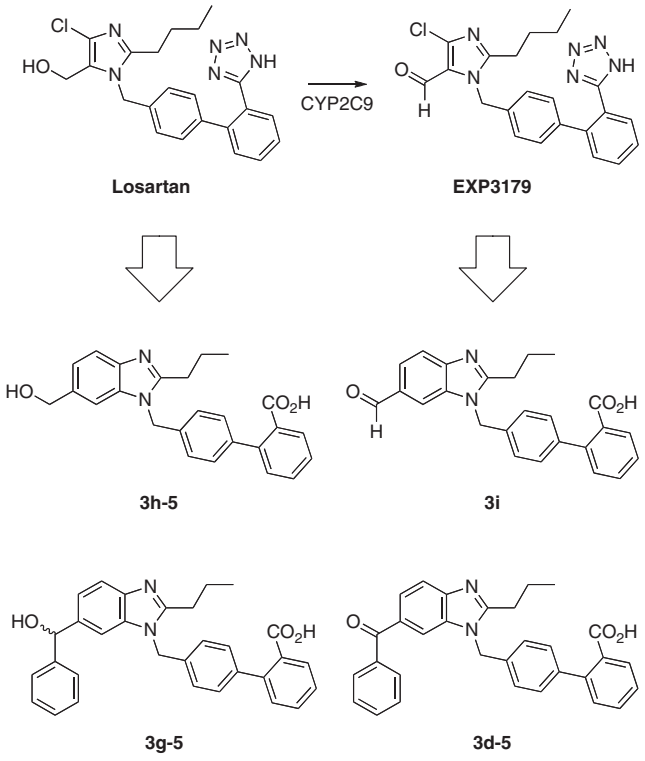

Figure 2. One step of Losartan metabolism and derivation of compounds **3d**–**5**, **3g**–**5**, **3h**–**5** and **3i**.

propyl group, was important for potency and activation.[13] In continuation of our studies we investigated the significance of the positions 5 and 6 of the benzimidazole for PPARγ modulating activity.

First hints on the meaning of these positions gave the results of our first structure–activity relationship (SAR) study: compounds with a benzimidazole at position 5 or 6 were less active than Telmisartan. An additional *N*-methyl group at this substituent led to PPARγ agonists even more potent than Telmisartan.[12] Therefore, we decided to evaluate the importance of these positions more detailed using also partial structures of Losartan and its metabolite EXP3179.[14,15] As depicted in Figure 2 and Table 1 bromine, carbinol and carbonyl derivatives were selected to study the hydrophobic interactions as well as possible H-donor and H-acceptor binding at the receptor. Bromine was favoured because of the large binding pocket (see 3D modelling SAR studies) and the higher hydrophobicity compared to chlorine and fluorine.

2. Results

2.1. Chemistry

Compounds **1a**–**1f** were commercially available. Cyclocondensation of the respective 1,2-benzenediamine (**1a**–**1f**) with trimethyl orthobutyrate by dropwise addition of concd HCl (Scheme 1) yielded the 2-propyl substituted benzimidazoles **2a**–**2f**. The products **3a**–**3g** were generated by N-alkylation of the benzimidazole derivatives **2a**–**2d** with 4′-(bromomethyl)biphenyl-2-carbonitrile in dry DMF and NaH, with a following nitrile saponification with KOH in ethylene glycol at 185 °C. Under these conditions a reduction of the carbonyl function to the hydroxyl group took place resulting in compound **3g**–**5**/**6**.

Prior to the N-alkylation yielding the compounds **3h**–**5/6** and **3i**, the intermediate **2e** was reduced with $LiAlH_4$ in dry THF at −10 °C, and the nitrile group of **2f** was converted to a formyl group with Ni–Al alloy (Raney Nickel) in formaldehyde at 95 °C.[16]

Finally, compound **5** was obtained in the same way starting with the cyclocondensation of 2,3-diaminonaphthalene with trimethyl orthobutyrate as described above (Scheme 2).[17]

Separation of the regioisomers was carried out by a combination of silica gel column chromatography and fractional crystallization. The separation failed in the case of compound **3i** (ratio of the 5- to the 6-regioisomer: 6:4), also using preparative HPLC. Compounds **3d**–**6** and **3g**–**6** could only be obtained as a 33% enriched 6-regioisomer. Compounds **3d**–**5** and **3g**–**5** were isomerically pure.

The assignment of the moieties to the position 5 or 6 (**3b**–**5/6**, **3d**–**5/6**, **3g**–**5/6** and **3h**–**5/6**) was performed by differential ^{1}H NMR Nuclear Overhauser Effect experiments (NOE-Diff), on the basis of a saturation transfer from the C-7 positioned proton (H-7) at the central benzimidazole to the benzylic methylene group (see Figs. S1–S16 at Supplementary data).

2.2. In vitro SAR studies

Compounds were evaluated for PPARγ activation in vitro. PPARγ is known as the 'master regulator' of adipocyte differentiation. Its activity closely correlates with the degree of differentiation analyzed by Oil Red O-staining. Therefore, 3T3-L1 pre-/adipocyte differentiation was chosen as an established model for the assessment of cellular PPARγ activation (absorption bar chart in Figs. 3B and 4B, concentrations of each compound: 1 and 10 μM; vehicle (**V**): DMSO; positive controls: Pioglitazone (**P**) and Telmisartan (**T**)). All test compounds were also investigated in a luciferase transactivation assay, using COS-7 cells transiently transfected with pGal4-hPPARγDEF and pGal5-Tk-pGL3 (Figs. 3A and 4A). Pioglitazone, as a full PPARγ agonist, was used as a positive control and its maximum activation was defined as 100%. The results of both assays are summarized in Table 1 (EC_{50}-values, percentage of maximum luciferase activation and maximum adipocyte differentiation). Additionally, a column with calculated log *D*-values (ACD/Chemsketch 3.6) at physiological pH 7.4 was included, which is helpful for interpretation of the receptor activity.

Table 1
Overview of the in vitro data of the compounds **3a**–**3i** and **5**

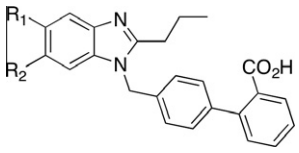

Compound[a]	R_1	R_2	*c*log *D* (pH 7.4)[b]	EC_{50}[c] (μM)	A_{max}[c] (%)	Max. diff. at 10 μM[d] (%)
Pioglitazone	—	—	2.06	0.14	100	100
Telmisartan	—	—	4.46	3.4	47	70
3a	H	H	2.37	1.9	49	67
3b–5	Br	H	3.01	0.4	104	103
3b–6	H	Br	3.03	0.47	79	102
3c	Br	Br	3.64	0.4	73	74
3d–5	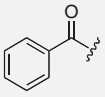	H	3.21	0.58	92	104
3d–6	H	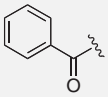	3.22	0.62	79	97
3g–5	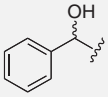	H	2.86	2.9	58	100
3g–6	H	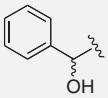	2.81	3.5	51	88
3i	Isomeric mixture of 5-/6-CH=O		1.68	10	37	45
5			3.61	0.26	109	105

[a] Compounds **3d–6** and **3g–6** were tested as isomeric mixtures. Compounds **3h–5**/**6** were inactive
[b] *c*log *D*-values were calculated with ACD/ChemSketch 3.6.
[c] Data for EC_{50} and maximum activation (A_{max}) values were taken from the graphs of Figures 3A and 4A, calculated with GraphPad Prism 4.
[d] Data for maximum differentiation values were taken from the bar chart of Figures 3B and 4B.

For the evaluation of the significance of the modifications compound **3a** was used for comparison. Its PPARγ activating property was described recently.[13]

Figure 3 illustrates the results of compounds **3a**, **3b–5**, **3b–6**, **3c** and **5** in the luciferase assay and the adipocyte differentiation assay. Compounds **3h–5** and **3h–6** showed no relevant effects (data not shown). If a bromine substituent is attached to compound **3a** in position 6 (**3b–6**), the lipophilicity rises from a *c*log *D* value of 2.37 (**3a**) to 3.03 (**3b–6**), which also led to a higher potency (EC_{50} = 0.47 μM). However the profile of a partial agonist as demonstrated for **3a** (max. activation of 49%) is shifted more to that of a full agonist (**3b–6** max. activation of 79%). Adipocyte differentiation reached 100%. The shift of the bromine substituent from position 6 to 5 (**3b–5**) increased the max. activation in the luciferase assay to 104% but let the potency nearly unchanged (EC_{50} = 0.4 μM). Compound **3c** with bromine substituents in both positions was more lipophilic (*c*log *D* = 3.64) and caused results (EC_{50} = 0.4 μM; max. activation of 73%) like **3b–6** in the luciferase assay. Replacing the benzimidazole scaffold of **3a** by an 1*H*-naphtho[2,3-*d*]imidazole yielded the most potent compound (**5**) in this series (EC_{50} = 0.26 μM; max. activation of 109%). The activation curve and the adipocyte differentiation behaviour were comparable to Pioglitazone.

It is obvious from the results depicted in Figure 4 that the efficacy is stronger in the case of benzophenone derivatives (**3d–5** and **3d–6**) compared to the carbinol congeners (**3g–5** and **3g–6**). The effect is nearly independent on the position (5 or 6) of the substituent: **3g–5** (EC_{50} = 2.9 μM, max. activation: 58%) < **3d–5** (EC_{50} = 0.58 μM, max. activation: 92%), **3g–6** (EC_{50} = 3.5 μM, max. activation: 51%) < **3d–6** (EC_{50} = 0.62 μM, max. activation: 79%). Replacement of the phenyl ring by H reduced the activity drastically: **3h–5**/**6** (no measurable activity, data not shown) < **3i** (**(**EC_{50} = 10 μM, max. activation: 37%).

With substituents at position 5 it is possible to reach a higher activation level than with those in position 6, keeping in mind that **3d–6**, **3g–6** and **3i** are isomeric mixtures. The concentration activity curves in the luciferase assay correlate well with the adipocyte differentiation assay, indicating a higher potency with a lower differentiation level for the 6 positioned compared to the 5 positioned moieties (Fig. 4B, Table 1). Because the binding mode of Telmisartan and related compounds is unknown we used these data and those of previous papers for 3D modelling SAR studies.

2.3. 3D modelling SAR studies

PPARγ is a challenging target for molecular modeling due to several reasons: (i) the active site is huge and consists of three arms of which only two have to interact with the ligand to show biological activity, (ii) the binding is considered flexible, that is, especially side chains are known to move significantly upon ligand binding, (iii) the binding site is highly lipophilic, which represents a challenge for structure-based approaches.[18–20] On the other

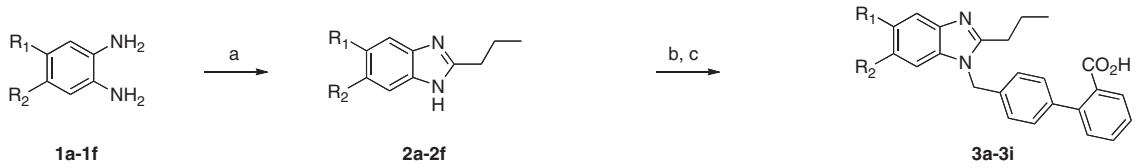

	R_1	R_2
1a	H	H
1b	H	Br
1c	Br	Br
1d	H	Phenylcarbonyl
1e	H	CO_2H
1f	H	CN

	R_1	R_2
2a	H	H
2b	H	Br
2c	Br	Br
2d	H	Phenylcarbonyl
2e	H	CO_2H
2f	H	CN

d, b, c

e, f, g

	R_1	R_2
3a	H	H
3b-5	Br	H
3b-6	H	Br
3c	Br	Br
3d-5	Phenylcarbonyl	H
3d-6	H	Phenylcarbonyl
3g-5	Hydroxy(phenyl)methyl	H
3g-6	H	Hydroxy(phenyl)methyl
3h-5	Hydroxymethyl	H
3h-6	H	Hydroxymethyl
3i	5-/6-Formyl (isomeric mixture)	

Scheme 1. Reagents and conditions: (a) $H_3C(CH_2)_2C(OCH_3)_3$, HCl, rt; (b) NaH, 4′-(bromomethyl)-2-biphenylcarbonitrile, DMF, 0 °C–rt; (c) ethylene glycol, KOH, 185 °C; (d) THF, $LiAlH_4$, −10 °C to rt; (e) Ni–Al, formaldehyde, H_2O, 95 °C; (f) NaH, methyl-4′-(bromomethyl)-2-biphenylcarboxylate, DMF, 0 °C–rt; (g) MeOH, aq NaOH soln (10%), reflux.

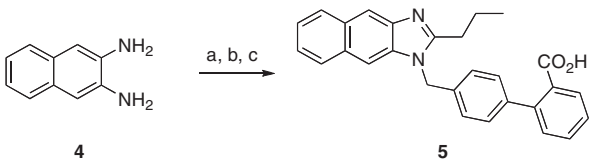

Scheme 2. Reagents and conditions: (a) $H_3C(CH_2)_2C(OCH_3)_3$, HCl, rt; (b) NaH, 4′-(bromomethyl)-2-biphenylcarbonitrile, DMF, 0 °C–rt; (c) ethylene glycol, KOH, 185 °C.

hand, there is a large amount of published experimental data and successful molecular modeling studies available. For example Chittiboyina et al. and Mizuno et al. published a study involving molecular docking to facilitate their research for Telmisartan analogs.[21,22] Their docking study was focused on a single ligand–PPARγ complex and relies on docking scores for compound ranking, while here several structures and pharmacophoric information are used to perform modeling studies.

55 PPARγ structures with different co-crystallized ligands have been deposited in the PDB at the time of submission of this paper. Moreover, several successful modeling applications for PPAR have been published that focus on known pharmacophoric patterns.[23–26] Based on this large amount of available experimental data, we were able to apply a more sophisticated docking work-flow.

In order to address the difficulties and to profit from the large amount of experimental data, 83 single chains were extracted from 55 partly polymeric PDB structures. For all of these chains, re-docking experiments were performed using CCDCs software GOLD.[28] If the ligand was geometrically placed within a root mean square deviation (RMSD) of below 4 Å to the co-crystallized conformation by the program, it was considered for further examination. From this set those structures were selected, in which the re-docked ligand showed the same chemical interactions as the experimentally

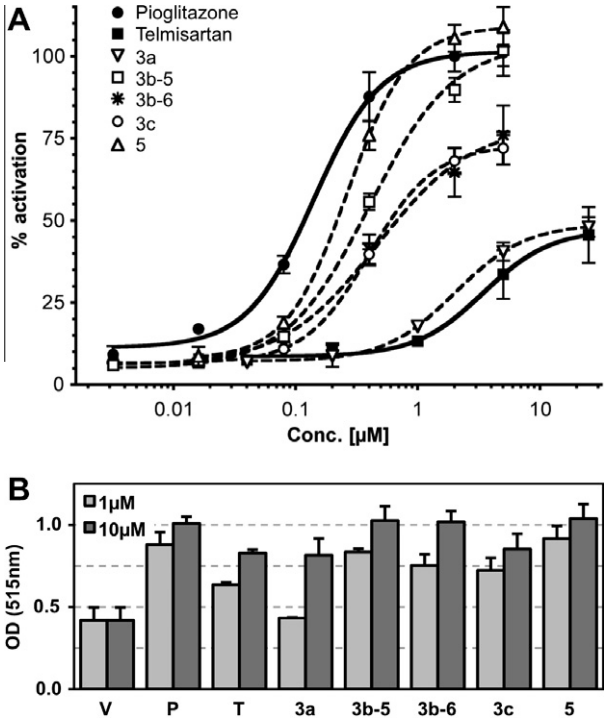

Figure 3. (A) Compounds tested in luciferase activation assay using COS-7 cells transiently transfected with pGal4-hPPARγDEF and pGal5-Tk-pGL3. Firefly luciferase activity was measured after 36 h and normalized with activity of cotransfected renilla luciferase. Points expressed are the means ± SD of threefold determination in a single experiment. Activation (%) of the luciferase gene in COS-7 cells by Pioglitazone (5 μM was defined as 100%), Telmisartan and the synthesized compounds **3a**–**3c** and **5**. (B) Lipid accumulation in 3T3-L1 cells after nine days of differentiation, ± the indicated compounds at 1 and 10 μM, was assessed by the quantification of Oil Red O after staining in isopropanol (OD_{515}). DMSO as vehicle (V), Pioglitazone (P) and Telmisartan (T) as positive controls.

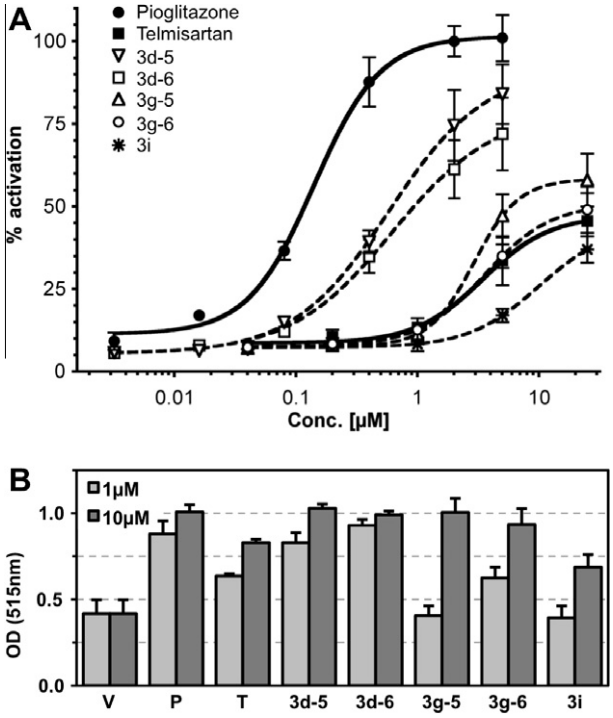

Figure 4. (A and B) Showing compounds **3d–5**, **3d–6**, **3g–5**, **3g–6** and **3i**. Methodical details are described in the legend of Figure 3.

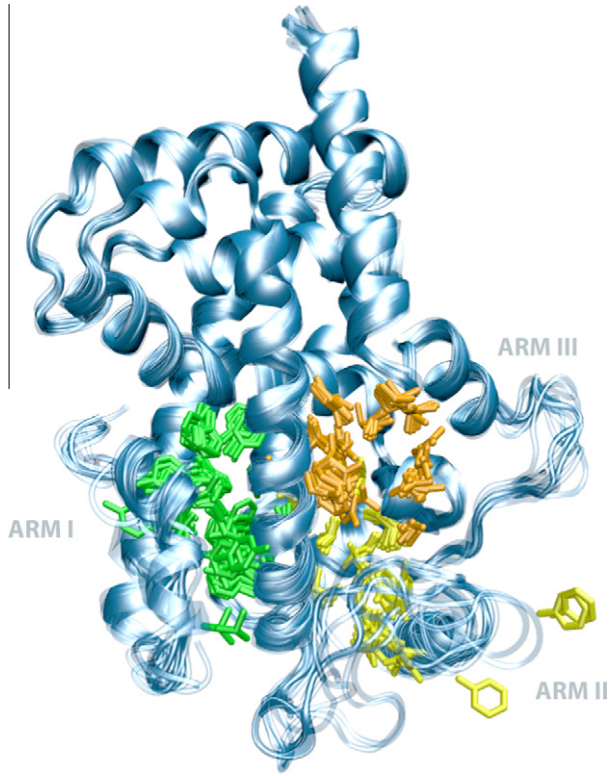

Figure 5. PDB structures as described in Table 2 after the backbone alignment procedure and removal of all ligands. Although the backbone can be overlaid without major deviations in most parts, there is still considerable side chain flexibility. Side-chains of arm I are colored in green, important arm II residues in orange, and arm III residues in yellow. Visualization was performed using VMD.[27]

determined pose. This procedure resulted in a high quality set of protein chains for subsequent docking experiments. Despite this quite restrictive selection, the chosen structures still cover a broad range of side chain movements and different ligand poses (Fig. 5). All resulting poses that fulfill all important pharmacophoric interactions were below 2 Å RMSD compared to the co-crystallized ligand (Table 2).

As a next step, the backbones of the isolated and selected chains were three-dimensionally aligned using the tool MUSTANG[29] in order to obtain a common coordinate frame. All compounds were docked into all of these aligned chains without further restrictions. Built-in scoring algorithms for ranking ligand poses are unapt to estimate binding energy, while it is common understanding that the resulting pose ensemble covers ligand conformational space in a reasonable way.[30]

Since Telmisartan was the lead structure for this study, we first tried to find an adequate binding mode for this compound. We compared all generated poses from the parallel docking experiments and selected the most plausible by visual inspection considering known important interactions from previous studies.[23] Telmisartan most likely forms hydrogen bonds to Ser342 at the carboxylic acid moiety, and shows at the same time a relevant charge transfer interaction with Arg288. These chemical features anchor the compound in arm II allowing hydrophobic contacts with Met348, Ile341, and Phe264. The central benzimidazole acts as a linker stabilizing the lipophilic parts of the molecule that point into arm I (Ile326, Leu469, Leu453) and arm III (Ala292, Leu333), so that the lipophilic part of the molecule can fill the hydrophobic portions of the pocket (Fig. 6). This predicted pose is in correspondence with the assumptions of Benson et al.,[10] although the charge transfer with Arg288 has not been described in detail. However, this interaction seems to be relevant, since also the endogenous PPARγ ligand alkylglycerophosphate was observed at this location.[31]

To further analyze and understand the mechanism of receptor activation by the synthesized compounds, a structure–activity relationship with a 3D pharmacophore-driven molecular modelling study has been performed. All the in vitro tested compounds from this (compounds **3a, 3b–5, 3b–6, 3c, 3d–5, 3d–6, 3g–5, 3g–6, 3i,** and **5**) and a former study (2-substituted benzimidazoles **4a–4j**) have been included[13] (compound **3a** is consistent with **4a**). From the pose shown in Figure 6, a three-dimensional pharmacophore model was derived using the software LigandScout.[32,33] All molecules were docked into the 12 selected structures and subsequently scored by a three-dimensional search using the Telmisartan 3D pharmacophore model built in LigandScout. The surmised binding poses are shown in Figure 7. Additionally, each resulting compound conformation is depicted separately in the Supplementary data.

Table 2
Selected PDB structures for docking experiments

PDB code	Chain identifier	RMSD (Å) of re-docked ligand
2fvj	A	0.83
2g0g	A	1.58
2g0h	B	0.44
2g0h	A	0.95
2om9	B	1.10
2om9	A	1.44
2om9	C	1.93
2q5s	A	0.46
2q61	B	1.17
2q6s	B	1.58
3b3k	A	0.87
4prg	A	1.42

All re-docked structures reproduce the important pharmacophoric interactions that can also be observed for the co-crystallized ligand.

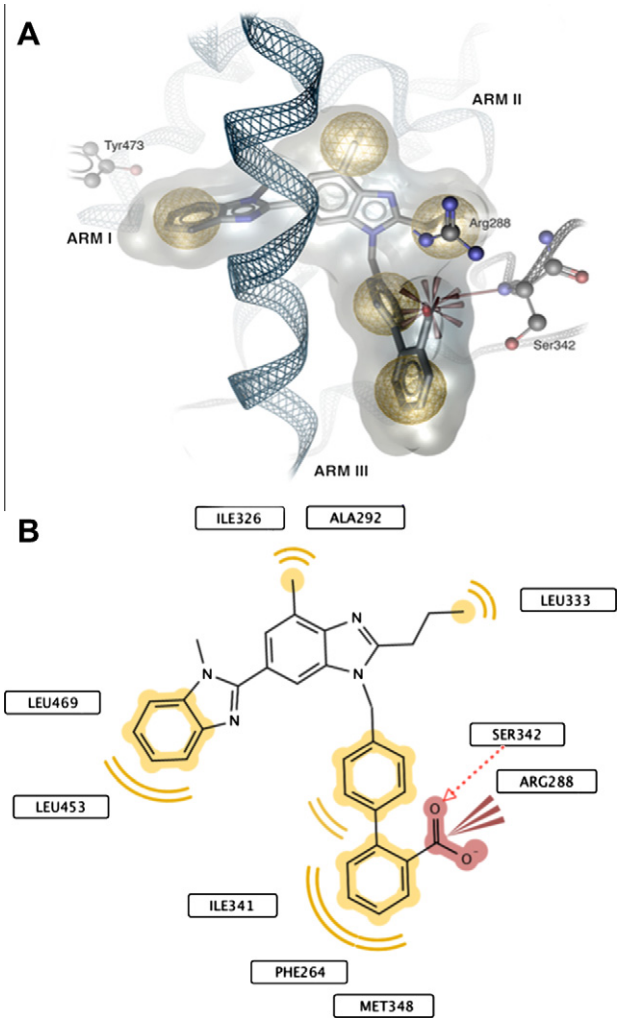

Figure 6. The putative binding mode of Telmisartan was used as a starting point. The LigandScout 3D pharmacophore consists of 5 lipophilic features (yellow spheres), a hydrogen bond (red arrow) and a charge transfer interaction (3D depiction on the top (A) and 2D illustration below (B) visualized with LigandScout).

2.3.1. SAR of position 2 of the central benzimidazole[13]

As mentioned above, alkyl chains such as propyl substituents at position 2 of the benzimidazole moiety are of special interest for potent PPAR agonists. Also other scaffolds for PPAR agonists containing such hydrophobic substituents have been published.[34,35] To rationalize the importance of propyl and other hydrophobic moieties at this position, we predicted the binding modes for compounds **4a**–**4j** (see Supplementary data) comprising different hydrophobic substituents at position 2. These binding poses explain the increase of activity from propyl to butyl (**4a** and **4b**) substituents, since the hydrophobic contact area is increased. The slight decrease in activity for compounds **4c** and **4d** could be related to hydrophobic contacts that can only be formed at the transition between arms I and III. Thus, the ligands cannot reach out to Tyr327 that interacts with **4a** and **4b**. The aromatic substitutions in **4e** and **4g** also permit lipophilic contacts with Met348, which leads to an increase in activity. The phenyl ring in compound **4f** shows an unfavorable conformation for the linear geometry of arm I and forms no hydrophobic contacts, whereas the chlorine substitution in compound **4h** can interact with Leu228 in arm III. The methoxy group in compound **4i** reaches out to arm III, potentially even forming a weak hydrophobic interaction with Tyr327.

An explanation for the decreased activity of phenol substitution in compound **4j** compared to the methoxyphenyl moiety of compound **4i** could be that the top scored pose is likely to trap a water molecule between the side chains of His323, His449, and Tyr473, which is entropically unfavorable. Although this hypothesis would have to be proved in more detailed theoretical studies, the geometry that was produced by rigid docking allows for plausible water placement using a simple MMFF94s force field minimization in LigandScout as shown in Figure 8.

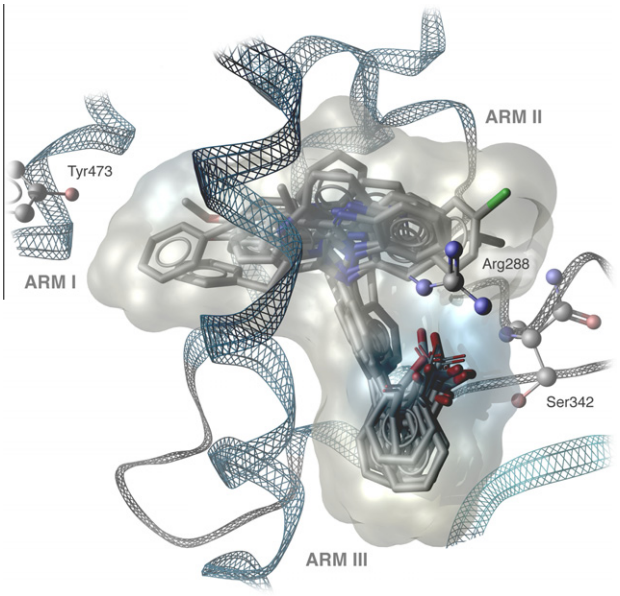

Figure 7. Overlay of structures **4a**–**4j** after parallel docking and 3D pharmacophore scoring in the PPARγ binding pocket (shown using PDB entry 2FVJ). All structures show the same anchoring point of the carboxylic acid moiety, while the lipophilic regions are mainly distributed between arms I and III.

2.3.2. SAR of positions 5 and 6 of the central benzimidazole

The increase in activity observed for the bromine substituted compounds **3b**–**5, 3b**–**6,** and **3c** in comparison to the unsubstituted compound **3a** can be easily explained by the rising lipophilicity and the larger area of hydrophobic contact possibilities. Compounds **3d**–**5** and **3d**–**6** both show a linear geometry that nicely binds into both arm I and III. The carbonyl group of the phenone moiety of **3d**–**5** not only forms hydrogen bonds to Tyr327, but also to Ser289 (Fig. 9), a PPAR residue which is known to be important for full agonistic activity.[18] The docking pose determined for **3d**–**6** is not able to form such hydrogen bonds. This could be an

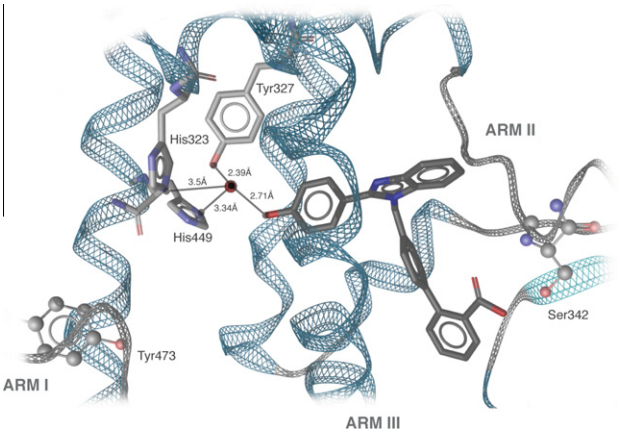

Figure 8. Compound **4j** potentially traps a water molecule between His323, His449, and Tyr327, which is entropically unfavourable. Red and green arrows indicate hydrogen bonding.

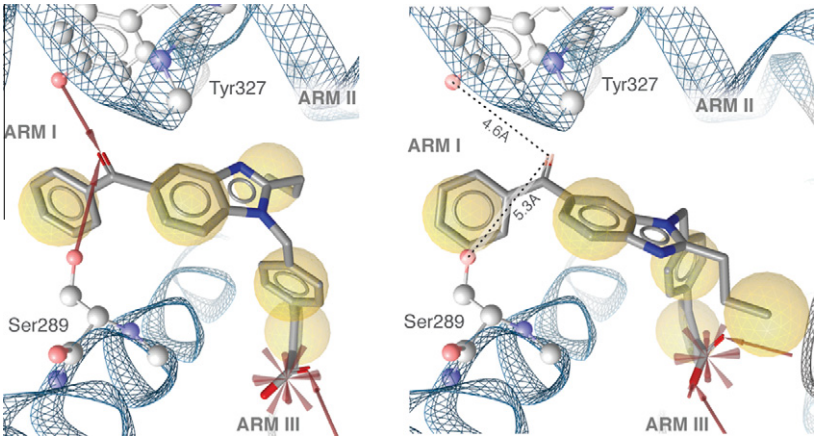

Figure 9. Compound **3d–5** (left) interacts with Tyr327 and Ser289 (illustrated by red vectors) resulting in full agonistic activity, while **3d–6** (right) cannot form these hydrogen bonds due to its different orientation.

explanation for the fact that in contrast to **3d–6**, **3d–5** acts as a full agonist.

The lack of biological activity determined for **3i** could not be explained by the docking studies in this work. One plausible explanation could be that the formyl moiety of **3i** acts as an 'electrophilic warhead', which could form a covalent bond with a residue located at the entrance of the PPAR ligand-binding pocket, such as known for PPARγ antagonists that bind covalently to Cys285.[36] Thus, compound **3i** could be forced into a conformation that does not allow proper ligand–protein interactions necessary for PPARγ activation. Compound **5**, finally, shows a perfect complementarity to the arm I/III binding pocket with a high degree of rigidity, which reflects its biological activity (Fig. 10). Each docking pose is provided as a separate image in the Supplementary data for further details.

3. Discussion and conclusion

In this SAR study some new benzimidazole derivatives could be characterized as PPARγ ligands and it has been shown that substituent changes at the 5- and 6-positions play a major role in receptor activation. On the one hand, the results demonstrate the importance of lipophilicity and on the other hand the direction of these positions, so that one could assume that the shift from position 6 to 5 leads from a partial to a full agonist. Thus, this needs to be elucidated in further studies. The partial to full agonism shift could also be seen for the exchange of the hydroxyl by a carbonyl function, that is, **3g–5**→**3d–5**, which could be explained by hydrogen bonds of the carbonyl oxygen with Tyr327 and Ser289. Above all, the rigidity and geometry of the structures have a positive influence on potency and maximum receptor activation, which is exemplified in the following row: **3g–6** < **3d–6** < **5**, where the most rigid compound **5** emerged as the most efficacious one (EC_{50} = 0.26 μM, max. activation: 109%), which could also be demonstrated in the modeling study.

The 3D pharmacophore-driven docking of both the 2-substituted and the 5/6-substituted benzimidazoles with the PPARγ correlated nicely with the in vitro data. It has been shown that a linear elongation with lipophilic moieties (**4e** and **4g**) results in better receptor activity. An interference of this linearity (**4f** and **4h**) decreased the activity, while a hydrophilic group (i.e., hydroxyl) in this position leads almost to inactivity (**4j**). Similar conclusions can be drawn for the 5/6-positioned substituents. These compounds only give a little insight to the possible opportunities of modulating the receptors activation by certain moieties (fine-tuning), which could be able to release a distinct conformational change and therefore a specific gene expression profile.

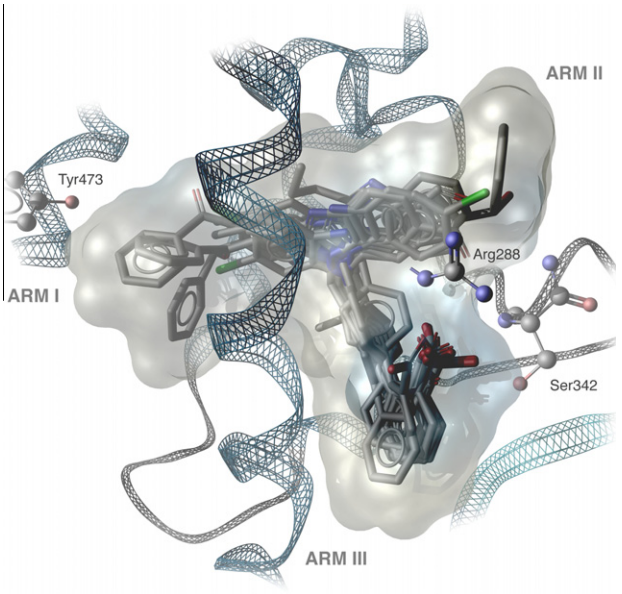

Figure 10. Overlay of structures **3a**, **3b–5**, **3b–6**, **3c**, **3d–5**, **3d–6**, **3g–5**, **3g–6**, **3i** and **5** in the PPARγ binding pocket. All structures show the same anchoring point of the carboxylic acid moiety, while the lipophilic regions are mainly distributed between arms I and III.

4. Experimental section

4.1. Chemistry

All reagents and solvents were purchased from Acros Organics, Sigma–Aldrich, Alfa Aesar or Merck. All reactions were monitored by TLC, performed on silica gel plates 60 F_{254} (Merck, Darmstadt/Germany). Visualization on TLC was achieved by UV light. Column chromatography was performed with Merck Silica Gel 60H, grain size <0.063 mm, 230 mesh ASTM (Darmstadt/Germany). Melting points: B 545 Büchi (Flawil/Schweiz) capillary melting point apparatus. ^{1}H NMR: Avance DPX-400 spectrometer (Bruker, Karlsruhe/Germany) at 400 MHz (internal standard: TMS). Elemental analyses: Microlaboratory of the Freie Universität Berlin with Elementaranalysator Vario EL (Elementar, Hanau); the analytical results are within 0.4% of theoretical values. EIMS spectra: CH-7A-Varian MAT, 70 eV (Melbourne/Australia). Microplate Reader FLASHScan S12 (Analytik Jena AG, Jena/Germany) Microlumat: Victor2 1420

Multilabel Counter (Wallac, Perkin–Elmer, Life sciences, Turku/Finnland).

Compounds **1a** (1,2-benzenediamine), **1b** (4-bromo-1,2-benzenediamine), **1c** (4,5-dibromo-1,2-benzenediamine), **1d** (3,4-diaminobenzophenone), **1e** (3,4-diaminobenzoic acid), **1f** (3,4-diaminobenzonitrile) were commercially available.

4.2. General procedure for the preparation of 2-substituted 1*H*-benzimidazoles

To a stirred suspension the appropriate 1,2-benzenediamine (10 mmol) in the trimethyl orthobutyrate (6.4 mL, 40 mmol) at room temperature concentrated HCl was added dropwise till the suspension was cleared up and started an exothermic reaction. A 5%-$NaHCO_3$ solution (50 mL) was transferred to the reaction mixture at pH 8 and extracted with $CHCl_3$ (3×25 mL). The organic layers were combined and dried over $NaSO_4$. After filtration, the solvent was removed under reduced pressure, and the resulting crude product was purified by chromatography on silica gel with CH_2Cl_2/methanol (95:5).

4.2.1. 2-Propyl-1*H*-benzo[*d*]imidazole (2a)

From 1,2-benzenediamine (1 g, 9.24 mmol) and trimethyl orthobutyrate (5.9 mL, 37 mmol). Colorless solid, 89%. ^{1}H NMR (DMSO-d_6): δ = 12.05 (s, 1H), 7.48–7.35 (m, 2H), 7.13–6.93 (m, 2H), 2.75 (t, J = 7.5 Hz, 2H), 1.77 (tq, J = 7.5 Hz, J = 7.4 Hz, 2H), 0.91 (t, J = 7.4 Hz, 3H).

4.2.2. 6-Bromo-2-propyl-1*H*-benzo[*d*]imidazole (2b)

From 4-bromo-1,2-benzenediamine (2 g, 10.7 mmol) and trimethyl orthobutyrate (6.9 mL, 43 mmol). Brown solid, 93%. ^{1}H NMR (DMSO-d_6): δ = 12.36 (s, 1H), 7.65 (s, 1H), 7.42 (d, J = 8.4 Hz, 1H), 7.24 (dd, J = 8.5 Hz, 1.9 Hz, 1H), 2.77 (t, J = 7.5 Hz, 2H), 1.77 (tq, J = 7.5 Hz, J = 7.4 Hz, 2H), 0.93 (t, J = 7.4 Hz, 3H).

4.2.3. 5,6-Dibromo-2-propyl-1*H*-benzo[*d*]imidazole (2c)

From 4,5-dibromo-1,2-benzenediamine (1 g, 3.76 mmol) and trimethyl orthobutyrate (3 mL, 18.8 mmol). Brown solid, 90%. ^{1}H NMR (DMSO-d_6): δ = 12.49 (s, 1H), 7.87 (s, 2H), 2.78 (t, J = 7.5 Hz, 2H), 1.77 (tq, J = 7.5 Hz, J = 7.4 Hz, 2H), 0.93 (t, J = 7.4 Hz, 3H).

4.2.4. Phenyl(2-propyl-1*H*-benzo[*d*]imidazol-6-yl)methanone (2d)

From 3,4-diaminobenzophenone (1 g, 4.7 mmol) and trimethyl orthobutyrate (3 mL, 18.8 mmol). Colorless solid, 85%. ^{1}H NMR of the tautomeric mixture (DMSO-d_6): δ = 12.61–12.54 (m, 1H), 7.89–7.80 (m, 1H), 7.75–7.72 (m, 2H), 7.69–7.63 (m, 2H), 7.60–7.55 (m, 3H), 2.87–2.80 (m, 2H), 1.87–1.76 (m, 2H), 0.99–0.93 (m, 3H).

4.2.5. 2-Propyl-1*H*-benzo[*d*]imidazole-6-carboxylic acid (2e)

From 3,4-diaminobenzoic acid (1 g, 6.57 mmol) and trimethyl orthobutyrate (4.2 mL, 26.3 mmol). Colorless solid, 94%. ^{1}H NMR of the tautomeric mixture (DMSO-d_6): δ = 12.68–12.54 (m, 1H), 12.55–12.47 (m, 1H), 8.10–8.00 (m, 1H), 7.78–7.73 (m, 1H), 7.58–7.46 (m, 1H), 2.85–2.77 (m, 2H), 1.84–1.75 (m, 2H), 0.98–0.92 (m, 3H).

4.2.6. 2-Propyl-1*H*-benzo[*d*]imidazole-6-carbonitrile (2f)

From 3,4-diaminobenzonitrile (1 g, 7.5 mmol) and trimethyl orthobutyrate (4.8 mL, 30 mmol). Colorless solid, 96%. ^{1}H NMR of the tautomeric mixture (DMSO-d_6): δ = 12.80–12.71 (m, 1H), 8.07–7.93 (m, 1H), 7.69–7.58 (m, 1H), 7.55–7.48 (m, 1H), 2.86–2.79 (m, 2H), 1.84–1.75 (m, 2H), 0.92–0.89 (m, 3H).

4.3. General procedure for N-alkylation with 4′-(bromomethyl)biphenyl-2-carbonitrile

To a stirred solution of the appropriate secondary amine (1 mmol) in dry DMF (3 mL) NaH (2 mmol) was added at 0 °C (ice cooling). After approx. 30 min (or after no more visible emergence of hydrogen) 4′-(bromomethyl)biphenyl-2-carbonitrile (0.3 g, 1.1 mmol) was added slowly and first stirred for 1 h at 0 °C and then 2–5 h at room temperature. The reaction mixture was poured in 6 N HCl (1 mL) with crushed ice (25 g) and extracted with $CHCl_3$ (3×15 mL). The organic layers were combined and dried over Na_2SO_4. After filtration, the solvent was removed under reduced pressure, and the resulting crude product was purified by chromatography on silica gel with stepwise gradient elution (CH_2Cl_2/methanol 99:1, 98:2, 95:5).

4.4. General procedure for saponification of carbonitriles

A stirred solution of the respective carbonitrile (1 mmol), KOH (0.28 g, 5 mmol) in H_2O (0.055 mL, 1 mmol) and ethylene glycol (4 mL) were heated at 185 °C. Every hour of the reaction time period some H_2O (1 mmol) has to be added cautiously. After 5–6 h the reaction mixture was cooled to 100 °C, and H_2O (8 mL) was added subsequently. The solution was acidified with 6 N HCl (pH 5–6) and stirred for 15 min to complete the precipitation. The obtained solid was purified by chromatography on silica gel with stepwise gradient elution (CH_2Cl_2/methanol 95:5, 9:1, 8:2) and recrystallization from methanol.

4.4.1. 4′-[(2-Propyl-1*H*-benzo[*d*]imidazol-1-yl)methyl]biphenyl-2-carboxylic acid (3a)

N-Alkylation of **2a** (0.5 g, 3.12 mmol) with 4′-(bromomethyl)biphenyl-2-carbonitrile (0.933 g, 3.43 mmol). The resulting 4′-[(2-propyl-1*H*-benzo[*d*]imidazol-1-yl)methyl]biphenyl-2-carbonitrile (91%, 1 g, 2.85 mmol) was treated with KOH (0.785 g, 14 mmol) as described for general procedure for saponification to give a colorless solid, 43% (39% total); mp: 255 °C; ^{1}H NMR (DMSO-d_6): δ = 12.74 (s, 1H), 7.69 (d, J = 7.7 Hz, 1H), 7.60–7.58 (m, 1H), 7.54–7.49 (m, 2H), 7.43 (t, J = 7.5 Hz, 1H), 7.33 (d, J = 7.7 Hz, 1H), 7.29 (d, J = 8.2 Hz, 2H), 7.18–7.16 (m, 2H), 7.12 (d, J = 8.1 Hz, 2H), 5.54 (s, 2H), 2.84 (t, J = 7.5 Hz, 2H), 1.79 (tq, J = 7.5 Hz, J = 7.4 Hz, 2H), 0.96 (t, J = 7.4 Hz, 3H); MS (EI, 225 °C): 370 [$M^{+\cdot}$]. Anal. Calcd for $C_{24}H_{22}N_2O_2$: C, 77.81; H, 5.99; N, 7.56. Found: C, 77.86; H, 6.17; N, 7.59.

4.4.2. 4′-[(5-Bromo-2-propyl-1*H*-benzo[*d*]imidazol-1-yl)methyl]-biphenyl-2-carboxylic acid (3b–5)

N-Alkylation of **2b** (1 g, 2.85 mmol) with 4′-(bromomethyl)biphenyl-2-carbonitrile (0.844 g, 3.1 mmol). After isomer separation on silica gel chromatography the resulting 4′-[(5-bromo-2-propyl-1*H*-benzo[*d*]imidazol-1-yl)methyl]biphenyl-2-carbonitrile (0.5 g, 1.16 mmol) was treated with KOH (0.325 g, 5.8 mmol) as described for general procedure for saponification to give a colorless solid, 73%; mp: 248 °C; ^{1}H NMR (DMSO-d_6): δ = 12.70 (s, 1H), 7.78 (d, J = 1.8 Hz, 1H), 7.69 (dd, J = 7.6, J = 1.2 Hz, 1H), 7.53 (td, J = 7.6, J = 1.4 Hz, 1H), 7.50–7.46 (m, 1H), 7.42 (td, J = 7.5, J = 1.2 Hz, 1H), 7.32–7.25 (m, 4H), 7.12–7.07 (m, 2H), 2.83 (t, J = 7.5 Hz, 2H), 1.75 (tq, J = 7.5 Hz, J = 7.4 Hz, 2H), 0.93 (t, J = 7.4 Hz, 3H); MS (EI, 180 °C): 448 [$M^{+\cdot}$]. Anal. Calcd for $C_{24}H_{21}BrN_2O_2$: C, 64.15; H, 4.71; N, 6.23. Found: C, 64.22; H, 4.97; N, 6.23.

4.4.3. 4′-[(6-Bromo-2-propyl-1*H*-benzo[*d*]imidazol-1-yl)methyl]-biphenyl-2-carboxylic acid (3b–6)

N-Alkylation of **2b** (1 g, 2.85 mmol) with 4′-(bromomethyl)biphenyl-2-carbonitrile (0.844 g, 3.1 mmol). After isomer separation on silica gel chromatography the resulting 4′-[(6-bro-

mo-2-propyl-1*H*-benzo[*d*]imidazol-1-yl)methyl]biphenyl-2-carbonitrile (0.5 g, 1.16 mmol) was treated with KOH (0.325 g, 5.8 mmol) as described for general procedure for saponification to give a colorless solid, 81%; mp: 258 °C; ^{1}H NMR (DMSO-d_6): δ = 12.71 (s, 1H), 7.81 (d, J = 1.8 Hz, 1H), 7.69 (dd, J = 7.8, J = 1.2 Hz, 1H), 7.55–7.51 (m, 2H), 7.42 (td, J = 7.5, J = 1.3 Hz, 1H), 7.33–7.27 (m, 4H), 7.12–7.02 (m, 2H), 5.54 (s, 2H), 2.79 (t, J = 7.5 Hz, 2H), 1.75 (tq, J = 7.5 Hz, J = 7.4 Hz, 2H), 0.93 (t, J = 7.4 Hz, 3H); MS (EI, 200 °C): 448 [M$^{+\cdot}$]. Anal. Calcd for $C_{24}H_{21}BrN_2O_2$: C, 64.15; H, 4.71; N, 6.23. Found: C, 64.10; H, 5.03; N, 6.43.

4.4.4. 4′-[(5,6-Dibromo-2-propyl-1*H*-benzo[*d*]imidazol-1-yl)-methyl]-biphenyl-2-carboxylic acid (3c)

N-Alkylation of **2c** (1 g, 3.15 mmol) with 4′-(bromomethyl)biphenyl-2-carbonitrile (0.944 g, 3.47 mmol). The resulting 4′-[(5,6-dibromo-2-propyl-1*H*-benzo[*d*]imidazol-1-yl)methyl]-biphenyl-2-carbonitrile (87%, 1.4 g, 2.75 mmol) was treated with KOH (0.772 g, 13.75 mmol) as described for general procedure for saponification to give a colorless solid, 81% (71% total); mp: 318 °C; ^{1}H NMR (DMSO-d_6): δ = 12.73 (s, 1H), 8.09 (s, 1H), 8.02 (s, 1H), 7.71 (dd, J = 7.7 Hz, 1.3 Hz, 1H), 7.55 (td, J = 7.6 Hz, J = 1.4 Hz, 1H), 7.44 (td, J=7.6 Hz, J = 1.3 Hz, 1H), 7.34 (dd, J = 7.7 Hz, J = 1.0 Hz, 1H), 7.31–7.28 (m, 2H), 7.11–7.07 (m, 2H), 5.57 (s, 2H), 2.81 (t, J = 7.5 Hz, 2H), 1.75 (tq, J = 7.5 Hz, J = 7.4 Hz, 2H), 0.93 (t, J = 7.4 Hz, 3H). MS (EI, 250 °C): 526 [M$^{+\cdot}$]. Anal. Calcd for $C_{24}H_{20}Br_2N_2O_2 \times 0.25H_2O$: C, 54.11; H, 3.88; N, 5.26. Found: C, 54.34; H, 4.01; N, 5.16.

The compounds **3d–5**, **3d–6**, **3g–5** and **3g–6** were prepared by general procedure for N-alkylation of **2d** (1.05 g, 4 mmol) with 4′-(bromomethyl)biphenyl-2-carbonitrile (0.944 g, 3.47 mmol). The resulting isomeric mixture (90%, 1.6 g, 3.6 mmol) of 4′-[(5-(phenylcarbonyl)-2-propyl-1*H*-benzo[*d*]imidazol-1-yl)methyl]-biphenyl-2-carbonitrile and 4′-[(6-(phenylcarbonyl)-2-propyl-1*H*-benzo[*d*]imidazol-1-yl)methyl]biphenyl-2-carbonitrile was treated with KOH (0.772 g, 13.75 mmol) as described for general procedure for saponification to give all four compounds as a colorless solid after silica gel column chromatography and recrystallization. For compounds **3d–6** and **3g–6** the isomeric ratio of the 5- to the 6-regioisomer is 4:6.

4.4.5. 4′-[(5-(Phenylcarbonyl)-2-propyl-1*H*-benzo[*d*]imidazol-1-yl)methyl]biphenyl-2-carboxylic acid (3d–5)

Colorless solid, 8% (7% total); mp: 216 °C; ^{1}H NMR (DMSO-d_6): δ = 12.74 (s, 1H), 7.95 (s, 1H), 7.77–7.65 (m, 6H), 7.59–7.52 (m, 3H), 7.44 (td, J = 7.6 Hz, 1.2 Hz, 1H), 7.36–7.30 (m, 3H), 7.17–7.12 (m, 2H), 5.62 (s, 2H), 2.88 (t, J = 7.5 Hz, 2H), 1.79 (tq, J = 7.5 Hz, J = 7.4 Hz, 2H), 0.97 (t, J = 7.3 Hz, 3H). MS (EI, 200 °C): 474 [M$^{+\cdot}$]. Anal. Calcd for $C_{31}H_{26}N_2O_3 \times 0.125H_2O$: C, 78.09; H, 5.55; N, 5.88. Found: C, 78.07; H, 5.78; N, 5.85.

4.4.6. 4′-[(5-/6-(Phenylcarbonyl)-2-propyl-1*H*-benzo[*d*]imidazol-1-yl)methyl]biphenyl-2-carboxylic acid (3d–6), isomeric ratio is 4:6

Colorless solid, 5% (4% total); ^{1}H NMR of the isomeric mixture (DMSO-d_6): δ = 12.49 (s, 1H), 7.97–7.93 (m, 1H), 7.77–7.49 (m, 9H), 7.46–7.41 (m, 1H), 7.35–7.31 (m, 3H), 7.18–7.11 (m, 2H), 5.62 (s, 2H), 2.96–2.87 (m, 2H), 1.86–1.77 (m, 2H), 1.01–0.95 (m, 3H). MS (EI, 200 °C): 474 [M$^{+\cdot}$]. Anal. Calcd for $C_{31}H_{26}N_2O_3 \times 0.25H_2O$: C, 77.72; H, 5.58; N, 5.85. Found: C, 77.91; H, 5.69; N, 5.73.

4.4.7. 4′-[(5-(Hydroxy(phenyl)methyl)-2-propyl-1*H*-benzo[*d*]imidazol-1-yl)methyl]biphenyl-2-carboxylic acid (3g–5)

Colorless solid, 9% (7% total); mp: 208 °C; ^{1}H NMR (DMSO-d_6): δ = 12.72 (s, 1H), 7.69 (dd, J = 7.7 Hz, J = 1.2 Hz, 1H), 7.57 (d, J = 1.4 Hz, 1H), 7.53 (td, J = 7.6 Hz, 1.4 Hz, 1H), 7.43 (dd, J = 7.6 Hz, J = 1.3 Hz, 1H), 7.41–7.38 (m, 3H), 7.32 (dd, J = 7.7 Hz, J = 0.9 Hz, 1H), 7.30–7.25 (m, 4H), 7.20–7.16 (m, 2H), 7.11–7.07 (m, 2H), 5.82 (d, J = 4.0 Hz, 1H), 5.78 (d, J = 4.0 Hz, 1H), 5.49 (s, 2H), 2.81 (t, J = 7.5 Hz, 2H), 1.75 (tq, J = 7.5 Hz, J = 7.4 Hz, 2H), 0.94 (t, J = 7.4 Hz, 3H). MS (EI, 300 °C): 476 [M$^{+\cdot}$]. Anal. Calcd for $C_{31}H_{28}N_2O_3$: C, 78.13; H, 5.92; N, 5.88. Found: C, 78.27; H, 6.14; N, 6.06.

4.4.8. 4′-[(5-/6-(Hydroxy(phenyl)methyl)-2-propyl-1*H*-benzo[*d*]imidazol-1-yl)methyl]biphenyl-2-carboxylic acid (3g–6), isomeric ratio is 4:6

Colorless solid, 5% (4% total); ^{1}H NMR of the isomeric mixture (DMSO-d_6): δ = 12.76 (s, 1H), 7.71 (td, J = 7.7 Hz, J = 1.2 Hz, 1H), 7.62–7.23 (m, 11H), 7.21–7.08 (m, 4H), 5.91–5.77 (m, 2H), 5.54–5.47 (m, 2H), 2.84–2.77 (m, 2H), 1.82–1.71 (m, 2H), 0.98–0.89 (m, 3H). MS (EI, 250 °C): 476 [M$^{+\cdot}$]. Anal. Calcd for $C_{31}H_{28}N_2O_3 \times 1.5H_2O$: C, 73.94; H, 6.20; N, 5.56. Found: C, 73.61; H, 6.15; N, 5.68.

4.4.9. 4′-[(5-(Hydroxymethyl)-2-propyl-1*H*-benzo[*d*]imidazol-1-yl)-methyl]biphenyl-2-carboxylic acid (3h–5) and 4′-[(6-(hydroxymethyl)-2-propyl-1*H*-benzo[*d*]imidazol-1-yl)methyl]biphenyl-2-carboxylic acid (3h–6)

To a stirred solution of **2e** (1 g, 4.9 mmol) in dry THF (30 mL) $LiAlH_4$ (0.56 g, 14.7 mmol) was added over 10 min under ice cooling. After stirring for 30 min on ice the reaction mixture was stirred at room temperature for 2 h and then heated under reflux for another 1 h. H_2O was added slowly till no more visible emergence of hydrogen was observed. After filtration, the solvent was removed under reduced pressure, and the resulting crude product was purified by chromatography on silica gel with stepwise gradient elution (CH_2Cl_2/methanol 98:2, 95:5). The resulting (2-propyl-1*H*-benzo[*d*]imidazol-6-yl)methanol (54%, 0.5 g, 2.63 mmol) was N-alkylated by general procedure with 4′-(bromomethyl)biphenyl-2-carbonitrile (0.79 g, 2.9 mmol). The resulting isomeric mixture of 4′-[(5-/6-(hydroxymethyl)-2-propyl-1*H*-benzo[*d*]imidazol-1-yl)methyl]biphenyl-2-carbonitrile (33%, 0.33 g, 0.87 mmol) was treated with KOH (0.244 g, 4.35 mmol) as described for general procedure for saponification to give a colorless solid. The 5-/6-regioisomers were separated by silica gel column chromatography.

Compounds **3h–5**: colorless solid, 31% (6% total); mp: 175 °C; ^{1}H NMR (DMSO-d_6): δ = 12.76 (s, 1H), 7.69 (d, J = 7.2 Hz, 1H), 7.54–7.50 (m, 2H), 7.44–7.40 (m, 2H), 7.34–7.27 (m, 3H), 7.14 (d, J = 8.3 Hz, 1H), 7.11–7.09 (m, 2H), 5.52 (s, 2H), 5.12–5.09 (m, 1H), 4.57 (d, J = 3.9 Hz, 2H), 2.83 (t, J = 7.4 Hz, 2H), 1.78 (tq, J = J = 7.5 Hz, J = 7.4 Hz, 2H), 0.96 (t, J = 7.3 Hz, 3H). MS (EI, 200 °C): 400 [M$^{+\cdot}$]. Anal. Calcd for $C_{25}H_{28}N_2O_5 \times 2H_2O$: C, 68.79; H, 6.47; N, 6.42. Found: C, 68.99; H, 6.36; N, 6.28.

Compounds **3h–6**: colorless solid, 22% (4% total); mp: 200 °C; ^{1}H NMR (DMSO-d_6): δ = 12.73 (s, 1H), 7.69 (d, J = 7.2 Hz, 1H), 7.56–7.51 (m, 2H), 7.46–7.40 (m, 2H), 7.33 (d, J = 8.3 Hz, 1H), 7.31–7.26 (m, 2H), 7.13 (dd, J = 8.3, J = 1.5 Hz, 1H), 7.11–7.07 (m, 2H), 5.52 (s, 2H), 5.16 (t, J = 5.1 Hz, 1H), 4.57 (d, J = 4.8 Hz, 2H), 2.81 (t, J = 7.5 Hz, 2H), 1.77 (tq, J = 7.5 Hz, J = 7.4 Hz, 2H), 0.95 (t, J = 7.3 Hz, 3H). MS (EI, 225 °C): 400 [M$^{+\cdot}$]. Anal. Calcd for $C_{25}H_{28}N_2O_5 \times 0.65H_2O$: C, 72.85; H, 6.19; N, 6.80. Found: C, 72.86; H, 6.41; N, 7.13.

4.4.10. 4′-[(5-/6-Formyl-2-propyl-1*H*-benzo[*d*]imidazol-1-yl)methyl]biphenyl-2-carboxylic acid (3i), isomeric ratio 6:4

To a solution of **2f** (1 g, 5.4 mmol) in 60 mL formic acid and 20 mL of H_2O, Ni–Al alloy (4 g) was added in several portions. The reaction mixture was heated at 95 °C for 4 h. The hot mixture was filtered with the aid of Celite and washed thrice with water. The solution was concentrated and the pH was adjusted to 9 by the dropwise addition of 2 N NaOH. The product was obtained by

extraction with CH_2Cl_2 (3 × 50 mL). The organic layers were combined, dried over Na_2SO_4, concentrated in vacuo and purified by silica gel column chromatography to give a colorless solid. The resulting 2-propyl-1*H*-benzo[*d*]imidazole-6-carbaldehyde (35%, 0.36 g, 1.89 mmol) was N-alkylated by general procedure with 4′-(bromomethyl)biphenyl-2-carbonitrile (0.57 g, 2.08 mmol). The resulting isomeric mixture of 4′-[(5-/6-formyl-2-propyl-1*H*-benzo[*d*]imidazol-1-yl)methyl]biphenyl-2-carbonitrile (84%, 0.6 g, 1.58 mmol) was treated with KOH (0.44 g, 7.9 mmol) as described for general procedure for saponification to give a colorless solid, 71% (21% total); ^{1}H NMR of the isomeric mixture (DMSO-d_6): δ = 12.73 (s, 1H), 10.05–10.01 (m, 1H), 8.20–8.15 (m, 1H), 7.80–7.69 (m, 3H), 7.55 (td, *J* = 7.6 Hz, *J* = 1.3 Hz, 1H), 7.44 (td, *J* = 7.6 Hz, *J* = 1.1 Hz, 1H), 7.35–7.27 (m, 3H), 7.21–7.09 (m, 2H), 5.68–5.61 (m, 2H), 2.92–2.81 (m, 2H), 1.85–1.75 (m, 2H), 0.99–0.94 (m, 3H). MS (EI, 200 °C): 398 [$M^{+\cdot}$]. Anal. Calcd for $C_{25}H_{28}N_2O_5 \times 0.75H_2O$: C, 72.89; H, 5.75; N, 6.80. Found: C, 72.94; H, 5.50; N, 6.71.

4.4.11. 4′-[(2-Propyl-1*H*-naphth[2,3-*d*]imidazol-1-yl)methyl]-biphenyl-2-carboxylic acid (5)

From 2,3-diaminonaphthalene (0.5 g, 3.2 mmol) and trimethyl orthobutyrate (2 mL, 12.8 mmol) as described for general procedure for the preparation of 2-substituted 1*H*-benzimidazoles. The resulting 2-propyl-1*H*-naphth[2,3-*d*]imidazol (94%, 0.63 g, 3 mmol) was N-alkylated by general procedure with 4′-(bromomethyl)biphenyl-2-carbonitrile (0.898 g, 3.3 mmol). The resulting 4′-[(2-propyl-1*H*-naphth[2,3-*d*]imidazol-1-yl)methyl]biphenyl-2-carbonitrile (88%, 1 g, 2.6 mmol) was treated with KOH (0.73 g, 13 mmol) as described for general procedure for saponification to give a colorless solid, 91% (74% total); mp: 271 °C; ^{1}H NMR (DMSO-d_6): δ = 12.71 (s, 1H), 8.15 (s, 1H), 8.04–7.97 (m, 2H), 7.96–7.92 (m, 1H), 7.70 (dd, *J* = 7.6 Hz, *J* = 1.1 Hz, 1H), 7.53 (td, *J* = 7.5 Hz, *J* = 1.2 Hz, 1H), 7.43 (td, *J* = 7.6 Hz, *J* = 1.1 Hz, 1H), 7.40–7.27 (m, 5H), 7.17 (d, *J* = 8.2 Hz, 2H), 5.64 (s, 2H), 2.92 (t, *J* = 7.5 Hz, 2H), 1.85 (tq, *J* = 7.5 Hz, *J* = 7.4 Hz, 2H), 1.00 (t, *J* = 7.4 Hz, 3H). MS (EI, 230 °C): 420 [$M^{+\cdot}$]. Anal. Calcd for $C_{28}H_{24}N_2O_2$: C, 79.98; H, 5.75; N, 6.66. Found: C, 80.14; H, 5.99; N, 6.62.

5. Biology

Telmisartan and Pioglitazone were obtained from the pharmacy extracted with $CHCl_3$ and purified by chromatography on silica gel and recrystallized from methanol.

5.1. Differentiation assay

Murine 3T3-L1 preadipocytes were cultured in DMEM (+10% FCS) and differentiated by a modified previously described protocol:[9] after two days postconfluent preadipocytes were treated for three days with complete medium containing 1 μM Dexamethasone and 0.17 μM insulin. After medium replacement they were incubated for further three days with insulin (0.17 μM), and for the last three days with only complete medium. Cells were treated the whole time period with either vehicle (DMSO) as negative control, Pioglitazone and Telmisartan as positive controls or the synthesized compounds until day 9 of differentiation, after which the cells were washed with phosphate-buffered saline and stained with Oil Red O.[9] For quantification, the dye was extracted with isopropanol (80% V/V) and the absorption was measured at 515 nm.

5.2. PPARγ transactivation assay

Transient transfection (Invitrogen) and luciferase assays (Promega) were performed as described in the manufacture protocol. COS-7 cells (8 × 10^5/well in a 96-well plate) were seeded the day before and transfected for each well with the use of 0.25 μL Lipofectamine 2000 (Invitrogen) with 4.5 ng pGal4-hPPARγDEF, 45 ng pGal5-TK-pGL3 and 3 ng pRL-CMV in 25 μL Opti-MEM (Gibco).[37] After 4 h, a sixth part of the transfection medium volume of DMEM (+10% FCS) plus the compounds or vehicle (DMSO) was added; luciferase activity was measured after 36 h.

Acknowledgements

This work was supported by Grants Gu 285/7–1/2 and Ki 712/3–1/2 from the Deutsche Forschungsgemeinschaft (DFG).

Supplementary data

Supplementary data associated with this article can be found, in the online version, at doi:10.1016/j.bmc.2010.06.102.

References and notes

1. Michalik, L.; Auwerx, J.; Berger, J. P.; Chatterjee, V. K.; Glass, C. K.; Gonzalez, F. J.; Grimaldi, P. A.; Kadowaki, T.; Lazar, M. A.; O'Rahilly, S.; Palmer, C. N.; Plutzky, J.; Reddy, J. K.; Spiegelman, B. M.; Staels, B.; Wahli, W. *Pharmacol. Rev.* **2006**, *58*, 726.
2. Spiegelman, B. M. *Diabetes* **1998**, *47*, 507.
3. Willson, T. M.; Brown, P. J.; Sternbach, D. D.; Henke, B. R. *J. Med. Chem.* **2000**, *43*, 527.
4. Berger, J.; Moller, D. E. *Annu. Rev. Med.* **2002**, *53*, 409.
5. Mangelsdorf, D. J.; Thummel, C.; Beato, M.; Herrlich, P.; Schütz, G.; Umesono, K.; Blumberg, B.; Kastner, P.; Mark, M.; Chambon, P.; Evans, R. M. *Cell* **1995**, *83*, 835.
6. Committee, N. R. N. *Cell* **1999**, *97*, 161.
7. Willson, T. M.; Wahli, W. *Curr. Opin. Chem. Biol.* **1997**, *1*, 235.
8. Berger, J. P.; Petro, A. E.; Macnaul, K. L.; Kelly, L. J.; Zhang, B. B.; Richards, K.; Elbrecht, A.; Johnson, B. A.; Zhou, G.; Doebber, T. W.; Biswas, C.; Parikh, M.; Sharma, N.; Tanen, M. R.; Thompson, G. M.; Ventre, J.; Adams, A. D.; Mosley, R.; Surwit, R. S.; Moller, D. E. *Mol. Endocrinol.* **2003**, *17*, 662.
9. Schupp, M.; Janke, J.; Clasen, R.; Unger, T.; Kintscher, U. *Circulation* **2004**, *109*, 2054.
10. Benson, S. C.; Pershadsingh, H. A.; Ho, C. I.; Chittiboyina, A.; Desai, P.; Pravenec, M.; Qi, N.; Wang, J.; Avery, M. A.; Kurtz, T. W. *Hypertension* **2004**, *43*, 993.
11. Schupp, M.; Clemenz, M.; Gineste, R.; Witt, H.; Janke, J.; Helleboid, S.; Hennuyer, N.; Ruiz, P.; Unger, T.; Staels, B.; Kintscher, U. *Diabetes* **2005**, *54*, 3442.
12. Goebel, M.; Clemenz, M.; Staels, B.; Unger, T.; Kintscher, U.; Gust, R. *ChemMedChem* **2009**, *4*, 445.
13. Goebel, M.; Staels, B.; Unger, T.; Kintscher, U.; Gust, R. *ChemMedChem* **2009**, *4*, 1136.
14. Schupp, M.; Lee, L. D.; Frost, N.; Umbreen, S.; Schmidt, B.; Unger, T.; Kintscher, U. *Hypertension* **2006**, *47*, 586.
15. Schmidt, B.; Schieffer, B. *J. Med. Chem.* **2003**, *46*, 2261.
16. Tawar, U.; Jain, A. K.; Dwarakanath, B. S.; Chandra, R.; Singh, Y.; Chaudhury, N. K.; Khaitan, D.; Tandon, V. *J. Med. Chem.* **2003**, *46*, 3785.
17. Narr, B.; Bomhard, A. D.; Hauel, N. D.; Van, D.; Jacques, M. EP Patent 0,392,317, 1990.
18. Markt, P.; Schuster, D.; Kirchmair, J.; Laggner, C.; Langer, T. *J. Comput. Aided Mol. Des.* **2007**, *21*, 575.
19. Cronet, P.; Petersen, J. F. W.; Folmer, R.; Blomberg, N.; Sjoblom, K.; Karlsson, U.; Lindstedt, E. L.; Bamberg, K. *Structure* **2001**, *9*, 699.
20. Xu, H. E.; Lambert, M. H.; Montana, V. G.; Parks, D. J.; Blanchard, S. G.; Brown, P. J.; Sternbach, D. D.; Lehmann, J. M.; Wisely, G. B.; Willson, T. M.; Kliewer, S. A.; Milburn, M. V. *Mol. Cell.* **1999**, *3*, 397.
21. Chittiboyina, A. G.; Mizuno, C. S.; Desai, P. V.; Patny, A.; Kurtz, T. W.; Pershadsingh, H. A.; Speth, R. C.; Karamyan, V.; Avery, M. A. *Med. Chem. Res.* **2009**, *18*, 589.
22. Mizuno, C. S.; Chittiboyina, A. G.; Patny, A.; Kurtz, T. W.; Pershadsingh, H. A.; Speth, R. C.; Karamyan, V. T.; Avery, M. A. *Med. Chem. Res.* **2009**, *18*, 611.
23. Markt, P.; Petersen, R. K.; Flindt, E. N.; Krjstiansen, K.; Kirchmair, J.; Spitzer, G.; Distinto, S.; Schuster, D.; Wolber, G.; Laggner, C.; Langer, T. *J. Med. Chem.* **2008**, *51*, 6303.
24. Xu, X. Y.; Cheng, F.; Shen, J. H.; Luo, X. M.; Chen, L. L.; Yue, L. D.; Du, Y.; Ye, F.; Jiang, S. H.; Zhu, D. Y.; Jiang, H. L.; Chen, K. X. *Int. J. Quantum Chem.* **2003**, *93*, 405.
25. Bharatam, P. V.; Patel, D. S.; Adane, L.; Mittal, A.; Sundriyal, S. *Curr. Pharm. Des.* **2007**, *13*, 3518.
26. Fracchiolla, G.; Laghezza, A.; Piemontese, L.; Carbonara, G.; Lavecchia, A.; Tortorella, P.; Crestani, M.; Novellino, E.; Loiodice, F. *ChemMedChem* **2007**, *2*, 641.
27. Humphrey, W.; Dalke, A.; Schulten, K. *J. Mol. Graphics* **1996**, *14*. 333-8, 27-8.
28. CCDC *Gold Suite*, Cambridge, UK, 2008.

29. Konagurthu, A. S.; Whisstock, J. C.; Stuckey, P. J.; Lesk, A. M. *Proteins* **2006**, *64*, 559.
30. Warren, G. L.; Andrews, C. W.; Capelli, A.-M.; Clarke, B.; LaLonde, J.; Lambert, M. H.; Lindvall, M.; Nevins, N.; Semus, S. F.; Senger, S.; Tedesco, G.; Wall, I. D.; Woolven, J. M.; Peishoff, C. E.; Head, M. S. *J. Med. Chem.* **2005**, *49*, 5912.
31. Li, Y.; Zhang, J.; Schopfer, F. J.; Martynowski, D.; Garcia-Barrio, M. T.; Kovach, A.; Suino-Powell, K.; Baker, P. R. S.; Freeman, B. A.; Chen, Y. E.; Xu, H. E. *Nat. Struct. Mol. Biol.* **2008**, *15*, 865.
32. Wolber, G.; Dornhofer, A. A.; Langer, T. *J. Comput. Aided Mol. Des.* **2006**, *20*, 773.
33. Wolber, G.; Langer, T. *J. Chem. Inf. Model.* **2005**, *45*, 160.
34. Santini, C.; Berger, G. D.; Han, W.; Mosley, R.; MacNaul, K.; Berger, J.; Doebber, T.; Wu, M.; Moller, D. E.; Tolman, R. L.; Sahoo, S. P. *Bioorg. Med. Chem. Lett.* **2003**, *13*, 1277.
35. Mahindroo, N.; Huang, C. F.; Peng, Y. H.; Wang, C. C.; Liao, C. C.; Lien, T. W.; Chittimalla, S. K.; Huang, W. J.; Chai, C. H.; Prakash, E.; Chen, C. P.; Hsu, T. A.; Peng, C. H.; Lu, I. L.; Lee, L. H.; Chang, Y. W.; Chen, W. C.; Chou, Y. C.; Chen, C. T.; Goparaju, C. M.; Chen, Y. S.; Lan, S. J.; Yu, M. C.; Chen, X.; Chao, Y. S.; Wu, S. Y.; Hsieh, H. P. *J. Med. Chem.* **2005**, *48*, 8194.
36. Leesnitzer, L. M.; Parks, D. J.; Bledsoe, R. K.; Cobb, J. E.; Collins, J. L.; Consler, T. G.; Davis, R. G.; Hull-Ryde, E. A.; Lenhard, J. M.; Patel, L.; Plunket, K. D.; Shenk, J. L.; Stimmel, J. B.; Therapontos, C.; Willson, T. M.; Blanchard, S. G. *Biochemistry* **2002**, *41*, 6640.
37. Raspé, E.; Madsen, L.; Lefebvre, A. M.; Leitersdorf, I.; Gelman, L.; Peinado-Onsurbe, J.; Dallongeville, J.; Fruchart, J. C.; Berge, R.; Staels, B. *J. Lipid Res.* **1999**, *40*, 2099.